Published in final edited form as:
Brain Stimul. 2013 January ; 6(1): 1–13. doi:10.1016/j.brs.2012.02.005.

Electric field depth–focality tradeoff in transcranial magnetic stimulation: simulation comparison of 50 coil designs

Zhi-De Deng[1,2], **Sarah H. Lisanby**[1,3], and **Angel V. Peterchev**[1,4,*]

Zhi-De Deng: zd2119@columbia.edu; Sarah H. Lisanby: sarah.lisanby@duke.edu; Angel V. Peterchev: angel.peterchev@duke.edu

[1]Department of Psychiatry and Behavioral Sciences, Duke University, Durham, NC, USA

[2]Department of Electrical Engineering, Columbia University, New York, NY, USA

[3]Department of Psychology and Neuroscience, Duke University, Durham, NC, USA

[4]Department of Biomedical Engineering and Department of Electrical and Computer Engineering, Duke University, Durham, NC, USA

Abstract

Background—Various transcranial magnetic stimulation (TMS) coil designs are available or have been proposed. However, key coil characteristics such as electric field focality and attenuation in depth have not been adequately compared. Knowledge of the coil focality and depth characteristics can help TMS researchers and clinicians with coil selection and interpretation of TMS studies.

Objective—To quantify the electric field focality and depth of penetration of various TMS coils.

Methods—The electric field distributions induced by 50 TMS coils were simulated in a spherical human head model using the finite element method. For each coil design, we quantified the electric field penetration by the half-value depth, $d_{1/2}$, and focality by the tangential spread, $S_{1/2}$, defined as the half-value volume ($V_{1/2}$) divided by the half-value depth, $S_{1/2} = V_{1/2}/d_{1/2}$.

Results—The 50 TMS coils exhibit a wide range of electric field focality and depth, but all followed a depth–focality tradeoff: coils with larger half-value depth cannot be as focal as more superficial coils. The ranges of achievable $d_{1/2}$ are similar between coils producing circular and figure-8 electric field patterns, ranging 1.0–3.5 cm and 0.9–3.4 cm, respectively. However, figure-8 field coils are more focal, having $S_{1/2}$ as low as 5 cm^2 compared to 34 cm^2 for circular field coils.

Conclusions—For any coil design, the ability to directly stimulate deeper brain structures is obtained at the expense of inducing wider electrical field spread. Novel coil designs should be benchmarked against comparison coils with consistent metrics such as $d_{1/2}$ and $S_{1/2}$.

[*]Corresponding author. Department of Psychiatry and Behavioral Sciences, Duke University, Box 3950 DUMC, Durham, NC 27710, tel. +1 919 684 0383, fax +1 919 681 9962, angel.peterchev@duke.edu.

Disclosure

Mr. Deng is inventor on patent applications and invention disclosures on TMS technology. Dr. Lisanby has served as Principal Investigator on industry-sponsored research grants to Columbia/RFMH or Duke (Brainsway, ANS/St. Jude Medical, NeoSync); equipment loans to Columbia or Duke (Magstim, MagVenture); is co-inventor on a patent application on TMS technology; is supported by grants from NIH (R01MH091083-01, 5U01MH084241-02, 5R01MH060884-09), Stanley Medical Research Institute, and National Alliance for Research on Schizophrenia and Depression; and has no consultancies, speakers bureau memberships, board affiliations, or equity holdings in related industries. Dr. Peterchev is inventor on patents and patent applications on TMS technology, including TMS technology licensed to Rogue Research; is Principal Investigator on a research grant to Duke from Rogue Research and equipment donations to Columbia (Magstim, ANS/St. Jude Medical); has received patent royalties from Rogue Research through Columbia; and is supported by NIH grant R01MH091083 and Wallace H. Coulter Foundation Translational Partners grant.

Keywords

transcranial magnetic stimulation; electric field; depth; focality; simulation

Introduction

Transcranial magnetic stimulation (TMS) is a non-invasive technique that is used or investigated for numerous research and therapeutic applications, including the study of normal and pathological brain function and the treatment of neurological and psychiatric disorders.[1,2] TMS uses brief, intense pulses of electric current delivered to a coil placed on the subject's head to generate an electric field in the brain via electromagnetic induction. The induced electric field modulates the neural transmembrane potentials and, thereby, neural activity. The locus of activation in the brain is approximately in the area where the induced electrical field is maximal[3,4]; this location, in turn, depends on the stimulating coil geometry and placement. For the purpose of determining a map of direct neural activation by TMS, the induced electric field distributions generated by different coil types have been characterized by theoretical calculations,[5–13] numerical simulation models,[14–21] and measurements of the electric currents induced in phantoms[22,23] or *in vivo*.[24,25] However, the analytic studies use idealized circular and/or figure-8 coil geometries, and only a handful of commercial coils have been modeled in computational studies.[21,26–28] Thus, electric field distribution data for many commercial or experimental TMS coils are still lacking. Knowledge of the electric field spatial distribution of specific coils and how it compares to other coils is valuable in the design and interpretation of basic research and clinical studies, as well as in the development of novel coils.

Two electric field spatial features of particular interest are depth of penetration and focality. Proposed or implemented coil designs have often been developed with the objective of improving one or both of these field characteristics. For example, in applications where the stimulation target is small (e.g., hand muscle representations in the primary motor cortex), localization of the induced electric field is important in order to minimize the stimulation of non-target regions. There has also been substantial interest in direct, non-invasive stimulation of brain regions deeper than the superficial cortex. For example, the subcallosal cingulate cortex, which lies approximately 6 cm from the head surface, is a putative target for the treatment of depression.[29,30] However, the design of TMS coils to stimulate such deep brain targets is limited by the rapid attenuation of the electric field in depth. It has been mathematically proven that at the quasi-static frequencies used in TMS the electric field is always stronger on the surface than inside of a spherically symmetric volume conductor.[31] Further, the electric field in the center of a uniformly conducting sphere is always zero.[10,13,32,33] Therefore, direct stimulation with TMS of regions near the center of the head appears impossible.

It is known that coils with larger dimensions generate an electric field that penetrates deeper but is less focal than that of smaller coils.[3,33–35] However, this electric field depth–focality tradeoff is not always acknowledged when novel TMS coil designs are proposed and has not been characterized with a uniform set of metrics. This is a serious limitation to clinical and basic neuroscience applications because stimulation of non-target brain regions may affect clinical outcomes, and certainly affects the degree to which any observed changes in behavior can be attributed to stimulation of the deep target alone rather than the neighboring regions that are also affected by the broader field. Furthermore, the electric field depth and focality may relate to risk of accidental seizure and other adverse side effects. Consequently, the safety guidelines for the use of repetitive TMS which are based on studies with ~70 mm

figure-8 coils[36] should be applied with caution to coil designs generating significantly different electric field characteristics.

The first TMS system used a circular coil (see, e.g., Figure 1(2, 4, 5)) due to its simple geometry and, hence, ease of construction.[37,38] However, the circular coil induces a nonfocal ring-shaped electric field maximum potentially stimulating a swath of brain regions under the coil perimeter. Attempts have been made to focalize the stimulation site with circular coils by introducing an angulated extension in the winding[39] or by modifying the winding density[40,41] or concavity.[42] These approaches, however, only marginally enhance the circular coil's ability to produce a focal field.[43] Thus far, the most significant improvement of TMS focality has been the introduction of the figure-8 coil (see, e.g., Figure 1(30, 31)), which has generally been credited to Ueno and colleagues,[44] although this coil configuration had been proposed earlier for the purpose of more localized sensing of magnetoencephalographic sources,[45] which is the inverse problem of focal TMS. The figure-8 configuration consists of a pair of adjacent circular loops with current flow in opposite directions, producing a relatively focal electric field maximum under the center of the coil where the two loops meet.[44] Cohen and Cuffin studied the focality of the figure-8 coil and found improvements with decreasing loop diameter down to 2.5 cm, at which point heating and stress limitations would necessitate sophisticated coil fabrication techniques.[32,46] Nevertheless, the search for even more focal TMS coils continues. The "cloverleaf" coil design consists of four sets of nearly circular windings (Figure 1(45)) and has been shown to be more efficient in stimulating long fibers compared to the figure-8 coil.[34,47–51] The "slinky" coil design consists of multiple circular or rectangular loops joined together at one edge and fanned out to form a half toroid (Figure 1(23, 24)).[12,52–55] Knäulein and Weyh introduced a figure-8 coil with eccentric windings producing higher density of winding turns toward the center of the coil than in the periphery (Figure 1(22)),[56] which has been shown to have better focality compared to the regular figure-8 and slinky coils of the same outer loop diameter.[57–59] The 3-D differential coil (Figure 1(41)) consists of a small figure-8 coil with a third loop positioned perpendicular to the center of the figure-8 coil and flanked by two additional loops to restrict the area of stimulation.[60] This 3-D differential coil has been shown to provide more focal stimulation compared to the figure-8 and slinky coils.[60,61] Other efforts to control the TMS electric field focality include the use of litz wire to construct small diameter figure-8 coils (Figure 1(21)),[62,63] conductive shielding plates (Figure 1(32)),[64–68] active shields (Figure 1(33)),[68,69] and ferromagnetic cores (Figure 1(3, 10, 11, 34, 40)).[28,70]

In parallel with the attempts to optimize the focality of magnetic stimulation, there have been efforts to increase the depth of stimulation. With conventional circular or figure-8 coils, the TMS-induced electric field is restricted to superficial cortical targets due to its rapid attenuation in depth. The double cone coil, formed by two large adjacent circular windings fixed at an angle (Figure 1(37)), has been shown to induce a more deeply penetrating and less focal electric field compared to a planar 70-mm figure-8 coil.[27] The double cone coil has been used for activation of the pelvic floor and lower limb motor representation at the interhemispheric fissure,[71] as well as transsynaptic activation of the anterior cingulate cortex via stimulation of the medial frontal cortex.[72] This coil is also highly efficient at seizure induction,[73] which is an advantage in the context of magnetic seizure therapy, but a potential source of risk in subconvulsive applications.

A family of coil designs called Hesed (H) coils has been proposed to achieve effective stimulation of deep brain structures.[74–77] The H coils have complex winding patterns and larger dimensions compared to conventional TMS coils, and consequently can be expected to have slower electric field attenuation with depth, at the expense of reduced focality. Measurements of the electric field induced by some H coils in a saline-filled phantom brain

reveal circular field patterns that are similar to those produced by large circular coils.[76] It has been proposed to use high-permeability ferromagnetic cores to improve the electric efficiency, field penetration, and focality of H coils.[78,79] The magnetic field associated with a particular coil design can be influenced by placing a ferromagnetic core within the field. However, the reported improvements from placing ferromagnetic cores in H coils were minor.[78,79] H coils are currently being evaluated for the treatment of a variety of psychiatric and neurological disorders, including major depression,[80–87] schizophrenia,[88,89] dystonia,[90] autism,[91] pain relief,[92] and chronic migraine.[93] However, the comparative advantage of H coils over conventional 70-mm figure-8 coils with regard to depth of stimulation has been disputed.[94–96] In addition, a randomized, sham-controlled, observer-blinded study in patients with benign essential blepharospasm has shown that the H coil used in that study has similar clinical effects to a 90-mm circular coil.[90]

Other designs for deep brain TMS coils have been proposed, such as the stretched C-shaped ferromagnetic core coil,[3,68,97] circular crown coil,[3] and large halo coil.[98] The halo coil has been shown to elicit lower limb and trunk muscle contractions in a cynomolgus monkey, suggesting that this coil design is capable of directly stimulating relatively deep brain regions.[99] The effects on the brain of low-field magnetic stimulation using MRI gradient coils have also been investigated.[100–102] These deep TMS and MRI coils have larger dimensions than conventional coils and H coils, and are expected to provide slower decay rate of the electric field with distance, at the expense of reduced focality.

Another line of work on improving magnetic stimulation targeting concerns the use of independently-controlled multi-channel coil arrays.[103–115] The major advantage of such a system is the flexibility of controlling the spatial electric field distribution and the ability to stimulate several brain areas simultaneously.[111] However, multi-channel arrays do not circumvent the fundamental limitations of electric field targeting.[31] Furthermore, high resolution targeting with multi-channel TMS requires small coil windings. Unfortunately, decreasing coil size is associated with higher electric losses, mechanical stress, and driving current.[9] The need for sophisticated control electronics further complicates the design. Another putative advantage of the independently-controlled multi-channel system is temporal summation of spatially distinct electric field pulses. Specifically, it has been proposed that the neuronal activation threshold in depth can be reduced relative to the superficial neural threshold by applying several consecutive pulses from a set of coils at different spatial locations.[77,116] However, our previous study showed theoretically that synchronous firing of all TMS coil channels is more effective for stimulating deep neurons than sequential firing.[3]

Understanding the electric field depth–focality tradeoff could help TMS clinicians and researchers with coil selection and interpretation of TMS studies, and can inform the selection of coil designs for magnetic seizure therapy. In the present paper we systematically compare the electric field penetration and focality for 50 commercial and experimental TMS coil designs in a spherical head model. Even though more anatomically accurate head models have been developed to reveal local detail of the TMS electric field and current density distribution,[17,19,117–121] the spherical model remains a useful reduction for parametric and comparative studies of global TMS coil characteristics such as electric field penetration and focality.[3,9,13,15,32–34,122] The results obtained with the spherical model are in reasonable agreement with a variety of quantitative and qualitative observations of TMS,[121,123–126] and are not limited to a particular subject's head anatomy or coil placement, which is an advantage for comparative studies of global TMS coil characteristics. Furthermore, the spherical model provides a standardized measure that can be easily replicated by various researchers evaluating coil designs.

This study has been presented in part in abstract form.[127]

Methods

Electric field simulation

The TMS coil and human head models, and the electric field solution were implemented with the finite element method package MagNet (Infolytica, Inc., Canada). The human head was modeled by a homogeneous sphere with 8.5 cm radius and isotropic conductivity of 0.33 S m^{-1}. The cortical surface was assumed to be at a depth of 1.5 cm from the surface of the head.[128] The distinct head tissue layers (scalp, skull, corticospinal fluid, and brain) were not differentiated, since magnetically induced electric field in a sphere is insensitive to radial variations of conductivity.[13]

We modeled 50 TMS coil configurations shown in Figure 1. In addition to modeling commercial coils from Brainsway (Jerusalem, Israel), Cadwell (Kennewick, WA, USA), Magstim (Whitland, Wales, UK), MagVenture (Farum, Denmark), and Neuronetics (Malvern, PA, USA), we have also included various coil designs proposed for enhancing the field focality or penetration. The MagVenture twin coil (Figure 1(36) and Figure 5) was modeled for various opening angles between the centers of the two loops to examine the effect of this parameter on the electric field depth–focality profile. The coils were modeled based on published data, manufacturer's specifications, coil X-rays, and inductance measurements. Detailed descriptions of the various coils are provided in Table S1 in the Supplementary Material. The minimum spacing between the coil windings and the surface of the head model was 5 mm to account for the thickness of the coil insulation. Ferromagnetic cores were modeled with a linear, homogeneous, isotropic material, with relative permeability of 1000 and electrical conductivity of 1 S m^{-1}.[79] Finally, we simulated the "flux ball" coil whose windings are parallel to the circles of latitude of the spherical model and cover the whole head (Figure 1, coil #0).[129] While this coil configuration is not physically realizable for brain stimulation, it illustrates the limiting case for large coils where the magnetic field intensity within the sphere becomes uniform, resulting in linear—the slowest possible—electric field attenuation in depth.[3,129]

Some clinical studies using H coils have not provided details of the coil geometry[90–93] or were published after the initial submission of this paper.[130] Since geometric details of these coils were not available to us for this study, these H coils were not modeled.

The electric field was computed with the 3-D electromagnetic time-harmonic solver of MagNet. MagNet first solves for the magnetic field **H** via the edge-element version of the T-Ω method.[131,132] Fields are assumed to be time-harmonic with angular frequency $\omega = 2\pi \times 5$ kHz. MagNet solves the equation

$$\nabla \times \left[(\sigma + j\omega\varepsilon)^{-1} \nabla \times \mathbf{H} \right] + j\omega\mu\mathbf{H} = 0 \quad (1)$$

where σ is the electrical conductivity, and ε and μ are electric permittivity and magnetic permeability of the medium, respectively. The tissue permeability was set to that of free space since head tissues are non-magnetic. The tissue permittivity was also set to that of free space since the quasistatic approximation is applicable to TMS[121] and since permittivity will not affect the normalized electric field depth and focality metrics used in this study, as discussed in the next section. The electric field was subsequently computed using Ampère's and Ohm's Laws

$$\mathbf{E}=\sigma^{-1}\nabla\times\mathbf{H}. \quad (2)$$

Electric field characterization

We compared the overall electric field distribution features of the various coils by plotting the field magnitude and direction on the brain surface (Figure 2).

We quantified the electric field penetration by the half-value depth, $d_{1/2}$, defined as the radial distance from the cortical surface to the deepest point where the electric field strength E is half of its maximum value on the cortical surface, $E_{\max}$.[133] The $d_{1/2}$ metric has units of length and quantifies the extent of the field along the radial brain dimension.

Focality is traditionally defined as the area where the electric field strength exceeds a certain value relative to the maximum at a given depth (e.g., the cortical surface). For example, the half-value area, $A_{1/2}$, is defined as the area of the cortex where the electric field exceeds half of the maximum electric field strength. Thus, focality quantifies the electric field spread in the two dimensions tangential to the brain surface. However, focality metrics such as $A_{1/2}$ are sensitive to the chosen surface depth where the area is calculated. Therefore, we adopted a more robust quantification of the electric field tangential spread, defined as

$$S_{1/2}=\frac{V_{1/2}}{d_{1/2}} \quad (3)$$

where $V_{1/2}$ is the half-value volume—the volume of the brain region that is exposed to an electric field as strong as or stronger than half of the maximum electric field.[123,133] Figure 3 illustrates the definitions of $d_{1/2}$ and $V_{1/2}$ for three different coils. Like $A_{1/2}$, the spread metric $S_{1/2}$ has units of area. The lower $S_{1/2}$, the more focal the electric field is. Collectively, $d_{1/2}$ and $S_{1/2}$ characterize the 3-D spatial extent of the TMS electric field.

The fraction of $E_{\max}$ relative to which the various depth and focality metrics are defined, typically $1/\sqrt{2}$,[60,61,65,66,79,134] 1/2,[33,122] or 1–1/ e,[135] is arbitrary and can be set to any value between 0 and 1 depending on the objectives of the evaluation. Furthermore, since the depth and focality metrics are normalized to the peak electric field, $E_{\max}$, they describe purely the relative spatial characteristics of the electric field and depend only on the coil geometry and placement. The peak electric field strength, as well as the pulse shape and width affect the focality of neural activation with TMS, but these parameters can be controlled by the pulse generation circuit of the TMS device and are therefore excluded from this characterization of the intrinsic spatial features of the coil electric field.[136]

Finally, the direction of the induced electric field in the brain is another important determinant of the effective stimulation strength and focality.[137–139] However, most TMS coils can be flexibly positioned and oriented on the head; therefore, the field direction relative to the brain is not an intrinsic property of the coil, but rather depends on the specific coil positioning. Therefore, we did not characterize the field direction as part of the intrinsic coil focality properties.

Results

Figure 2 shows the induced electric field distribution on the brain surface. Symmetric circular type coils (#1–7, 15, 16, 19, and 20) induce a single loop of eddy current with axial symmetry around the coil central axis. The H coils (#8–14), asymmetric crown coils (#17,

18), circular coil array (#46), and reverse current figure-8 coil (#47) produce electric field distributions similar to the single loop pattern of the circular coils. Symmetric figure-8 type coils (#21–26, 28, 29, 31, 32, 34–40) induce two loops of eddy current with reflection symmetry with respect to the *x-z* and *y-z* planes. The asymmetric figure-8 coils (#27, 30), coils arrays #42–44, and active shield figure-8 coil (#33) produce electric field distributions similar to those of the symmetric figure-8 coils. The 3-D differential coil (#41), cloverleaf coil (#45), active shield figure-8 coil (#48), MRI z-gradient coil in opposing-current mode (#49), and MRI x- (or y-) gradient coil (#50) produce more complex electric field distributions with multiple eddy current loops. Finally, the flux ball coil (#0) produces a broad, circular, symmetric electric field distribution.

Figure 4 shows the TMS electric field half-value spread $S_{1/2}$ as a function of the half-value depth $d_{1/2}$ for the 50 simulated TMS coils. The solid and dashed lines are curves of best fit of the points corresponding to the symmetric circular (#1–7, 15, 16, 19, and 20) and figure-8 (#21–26, 28, 29, 31, 32, 34–40) type coils, respectively. Coils #34* and #40*—are the air-core counterparts (core relative permeability set to 1) to ferromagnetic-core coils #34 and 40, respectively. The TMS coils exhibit a wide range of $S_{1/2}$ and $d_{1/2}$, but, as expected, are all subject to a depth–focality tradeoff. The range of $d_{1/2}$ is similar between the simulated circular and figure-8 type coils, 1.0–3.5 cm and 0.9–3.4 cm, respectively. However, figure-8 type coils are more focal compared to circular type coils, with $S_{1/2}$ range of 5–261 cm^2 and 34–273 cm^2, respectively. For either circualr or figure-8 type coils with $d_{1/2} < 2$ cm, $S_{1/2}$ and $d_{1/2}$ follow approximately a power law demonstrated by their near linear relationship on the logarithmic axes plot in Figure 4. Coils with deeper electric field penetration cannot be as focal as more superficial coils. Figure S1 in the Supplementary Material shows analogous plots of $V_{1/2}$ and $A_{1/2}$ versus $d_{1/2}$, demonstrating consistent depth–focality tradeoff for these alternative focality metrics as well.

The focality advantage of figure-8 over circular type coils diminishes as the $d_{1/2}$ increases. The depth–focality tradeoff curves for both coil types converge to the flux ball (coil #0) characteristics which correspond to linear electric field decay from the circles of latitude to the sphere axis where the field is zero.[3] Therefore, the maximum achievable $d_{1/2}$ is half the brain radius, 3.5 cm in our model (see Figure 4). The maximum $S_{1/2}$ is 308 cm^2, representing the most unfocal coil configuration possible. The most focal circular type coil is the mini-coil (#1) designed for stimulation in non-human primates, with $d_{1/2}$ and $S_{1/2}$ of 1.0 cm and 34 cm^2, respectively. The most focal figure-8 type coil is the three-layered double coil (#21), with $d_{1/2}$ and $S_{1/2}$ of 0.9 cm and 5 cm^2, respectively.

Developed for deep brain TMS, the H coils (#8–14) have relatively nonfocal, near circular electric field distribution. The H coils have deeper electric field penetration ($d_{1/2}$ = 1.7–2.4 cm) compared to conventional circular coils (e.g., #4–7, 15; $d_{1/2}$ = 1.4–1.9 cm). Larger diameter circular coils (e.g., #16–19, $d_{1/2}$ = 2.5–2.7 cm), in turn, produce more deeply penetrating electric field than H coils, at the expense of reduced focality. Large double-cone type coils (#36, 39) provide deeper stimulation ($d_{1/2}$ = 2.5–3.1 cm) than H coils with comparable or better focality.

The insertion of a ferromagnetic core in a coil can alter the focality and depth of the electric field, but is not able to circumvent the depth–focality tradeoff limits observed for air core coils. The effects of inserting a cylindrical ferromagnetic core (#3) through the center of a 50-mm circular coil (#2) are minor, reducing $d_{1/2}$ and $S_{1/2}$ by 3% and 5%, respectively. Placing a ferromagnetic core lateral to a circular coil can increase the field focality without sacrificing half-value depth. For example, adding a partial cylindrical core frontal (#10) or lateral (#11) to the H1 coil (#9) reduces $S_{1/2}$ by 6% and 0.8% while increasing $d_{1/2}$ by 5% and 1.4%, respectively. However, the resultant depth and focality are still inferior to the

performance of comparable figure-8 type coils. When a C-shaped ferromagnetic core (#34) is added to a figure-8 coil (#34*), both $d_{1/2}$ and $S_{1/2}$ are increased by 13% and 34%, respectively. On the other hand, adding a stretched C-core (#40) to a partial toroidal coil (#40*) reduces both $d_{1/2}$ and $S_{1/2}$ by 11% and 46%, respectively.

Finally, Figure 5 shows the electric field $S_{1/2}$ and $d_{1/2}$ profile for the twin coil for opening angles ranging from 90° to 180°. The field characteristics for a circular coil identical to one of the twin coil windings are plotted for comparison. The spread $S_{1/2}$ of the twin coil increases monotonically as the inter-loop opening angle widens. However, $d_{1/2}$ increases for opening angles from 90° to 110°, and decreases for opening angles from 110° to 180°. The focality locus in Figure 5 is replicated with a dotted line in Figure 4 for comparison with the other coils.

Discussion

Electric field depth–focality tradeoff

Among the TMS coil designs, there is a tradeoff between electric field depth of penetration and focality, as illustrated in Figure 4 and Figure S1 in the Supplementary Material. In general, coils with larger dimensions produce electric field with greater $d_{1/2}$ and $S_{1/2}$. In contrast, smaller coils produce electric field that is more localized and superficial. For conventional and smaller coil sizes ($d_{1/2}$ < 2 cm), $S_{1/2}$ and $d_{1/2}$ are related approximately by a power law for either circular or figure-8 type coils. It is noteworthy that none of the coil designs was able to overcome the depth–focality tradeoff set by the figure-8 type coils—no TMS coil performance lies significantly to the right of the dashed curve in Figure 4. This finding supports the claim that the figure-8 coil focality can only be modified somewhat but not improved substantially.[32] Hence, no TMS coil can achieve deep and focal stimulation simultaneously, consistent with previous findings.[31,33]

In this work we used a fixed size spherical model with radius of 8.5 cm. Variation in head anatomy could affect the electric field depth of penetration and focality. We have previously investigated the sensitivity of the induced electric field to anatomical variability (variation in head diameter, scalp and skull thickness, brain volume, and tissue electrical properties) in the context of magnetic seizure therapy.[140] The metrics $d_{1/2}$ and $S_{1/2}$ are most sensitive to the head diameter, but considered as percentage of their maximum values, which are head diameter dependent, they both scale similarly with head size. Furthermore, variability in head size is equivalent to variation in coil size for fixed head size, which is already illustrated in Figure 4. Therefore, variation in head anatomy would not change qualitatively the relative performance of the different coils.

This study focused on a comparison of the geometric characteristics of the electric field induced by various TMS coils. It did not characterize the effect of coil current waveform and amplitude, coil placement relative to anatomical head landmarks, and neural activation thresholds. Clearly these aspects of stimulation have to be considered in a more complete analysis of the extent of neural activation by TMS. In previous modeling studies of TMS we have considered the coil current waveform and amplitude and the neural response threshold.[123,140] Anatomically realistic TMS models[120,121] can be particularly useful in studying the effect of the complex tissue structure of the head on the electric field for various coil placements.

Strategies for controlling electric field focality

Several strategies have been deployed for making the electric field more focal. As illustrated in Figure 4 and Figure S1, a figure-8 type coil is always more focal than a circular type coil with the same $d_{1/2}$. The figure-8 type coil maintains its focality advantage over the circular

type coil of the same diameter as long as the two windings of the figure-8 remain relatively close.[34] For example, as illustrated in Figure 5, $S_{1/2}$ of the twin coil (#36) increases as the inter-loop opening angle increases, exceeding that of a single loop for angles above 103°.

Focality can be enhanced by reducing the diameter of the coil windings; smaller coils are more focal because the magnetic flux is more confined. The most focal of the circular and figure-8 type coils are the animal mini-coil (#1) and the 3-layer double coil (#21), respectively, both having a mean loop diameter of approximately 2 cm, approaching the smallest practical diameter.[46] It should be noted, however, that some of the smallest simulated coils were not designed for human cortical stimulation; coils #1, 6, and 25 were specifically designed for animal TMS where the electric field focality diminishes due to the smaller head size of animals.[141] Very small coils may be impractical for human TMS since they require excessively high currents to achieve threshold-level brain stimulation, because of the rapid attenuation of the electric field in depth.[9] Finally, different effective diameter of the coil windings contributes to differences between commercial coils with otherwise comparable specifications. For example, comparing two common “70 mm” figure-8 coils—the Magstim 70-mm figure-8 (#31) and the MagVenture B70 butterfly (#30)—show that $S_{1/2}$, $A_{1/2}$, and $d_{1/2}$ of the MagVenture coil are 6%, 8%, and 4% smaller compared to the Magstim coil which has a larger average winding diameter, consistent with the findings of previous comparisons of these two coils.[26]

Another approach to improve field focality is to concentrate the coil windings over the target area while distributing the return current paths away from the target. For example, in the case of the slinky coil (#23 and 24) the windings are fanned out while maintaining tangency of all the windings along one edge. Similarly, the focality of the crown coil (#16) can be improved by spreading (#17) or shifting (#18) the return paths away from the target. The eccentric figure-8 coils (#22 and #38) achieve improved focality in a similar fashion.

Various shielding strategies have been proposed for the improvement of TMS coil focality. Conductive plates (passive shields) or ancillary powered windings (active shields) could be used to create secondary fields that block the main coil field outside the region of interest. These techniques are widely applied in the design of MRI scanners.[142] By attaching a passive shield (#32) or an active shield with an appropriate number of turns (#33) to the 70-mm figure-8 coil (#31), $d_{1/2}$ decreases by 16% and 24% and $S_{1/2}$ decreases by 35% and 41%, respectively. Although similar reductions in $S_{1/2}$ and $d_{1/2}$ can be achieved by using smaller figure-8 coils (e.g., #25, 26), the shields provide more flexibility since a range of field characteristics can be obtained by tuning the conductive plate geometry or the current amplitude in the shielding coil without the need to modify the stimulation coil itself.[69] Shielding the coil could, however, increase losses due to the added conductive paths and reduce inductance which may affect the stimulator operation. Furthermore, some active shield configurations could reduce the coil focality—compare coil #48 with coils #31 and 33.

The insertion of a ferromagnetic core can increase or decrease to varying degrees the focality and depth of the electric field. For example, inserting a cylindrical ferromagnetic core through the center of a small circular coil (coil #3 versus #2) marginally increases focality but reduces stimulation depth. Placing a ferromagnetic core over one side of the winding in an H-coil with a circular type electric field pattern (coils #10 and 11 versus #9) enhances the magnetic flux and electric field under the core, similarly to the field concentration under the center of figure-8 type coils, consequently decreasing $S_{1/2}$ and increasing $d_{1/2}$ up to about 6%. Inserting ferromagnetic cores in figure-8 coils can have different effects on the depth–focality profile depending on the coil geometry. A C-shaped ferromagnetic core increases both $d_{1/2}$ and $S_{1/2}$ in coil #34 versus coil #34*, but reduces

both $d_{1/2}$ and $S_{1/2}$ in coil #40 versus #40*. Importantly, there does not appear to be a way of using ferromagnetic cores to improve the focality of figure-8 type coils beyond the depth–focality tradeoff curve associated with air-core figure-8 coils.

Given the vast number of possible multi-winding coil configurations, in this study we only examined a handful of them (coils #41–50). Some of the 3-D coil arrays (#42–44) display electric field characteristics similar to symmetric figure-8 coils with focality and depth comparable to medium/small size coils such as the MagVenture B65 (#29) or the Cadwell Corticoil (#26). The reverse-current figure-8 (#47), intended for sham TMS, exhibits circular electric field characteristics, since the opposing winding current directions at the coil center cancel the electric field there. The increased $d_{1/2}$ and $S_{1/2}$ indicate potential disadvantages of the use of current reversal in figure-8 coils for sham TMS.[143] The 3-D differential coil (#41), designed for very focal stimulation,[60] is indeed the most superficial of the simulated coils but the $S_{1/2}$ is inferior to that of small figure-8 coil. However, by the half-power area focality metric, $A_{1/\sqrt{2}}$, the 3-D differential coil has greater focality compared to the figure-8 and slinky coils,[60] demonstrating that the relative advantages of coil designs are in some cases dependent on the focality metric definitions. Similar observations apply to the cloverleaf coil (#45). Finally, other coils, such as the MRI gradient coils (#49 and 50) produce even more nonfocal stimulation than circular coils, which may have therapeutic applications.[102]

Strategies for controlling electric field depth

In this study we modeled all H coil designs used in clinical studies and published before the initial submission of this paper. H coil designs used in some recent studies[90–93,130] have winding geometries that can be classified as figure-8 type (Zangen A 2012, personal communication, Feb. 23, 2012) and may therefore have different depth–focality characteristics compared to the H coils modeled in this study.

Our results indicate that the modeled H coils (#8, 9, 12–14) have depth–focality characteristics consistent with large circular coils (see Figure 4). Therefore, $d_{1/2}$ of the H coil is smaller compared to figure-8 type coils with similar focality. Conversely, for a given $d_{1/2}$, the H coils induce a more diffuse field than figure-8 type coils. Some studies have indicated that H coils have significantly deeper field penetration than a conventional figure-8 coil. Specifically, at a depth of 4.5 cm, the electric field strength of the H1 and H2 coils is reported to be 66% and 81% of the maximal field induced at the surface of the skull, respectively, compared to 12% for the 70-mm figure-8 coil.[76,82] Furthermore, at 150% of motor threshold, the H2 coil reportedly enables effective activation of the medial prefrontal and subcortical frontal brain regions down to depth of 7 to 8 cm below the skull, compared to 2.5 cm for the figure-8 coil.[76] These results are based on electric field calculations along a lateral superior–inferior line in the brain and peak electric field measurements on transverse slices in a saline head phantom, but not on radial distance from the brain surface that is used in our definition of depth. Characterization of the field penetration by a distance that is not purely radial results in the electric field tangential spread contributing to the apparent depth of the field, thus confounding coil comparisons. Indeed, our results indicate a more moderate $d_{1/2}$ advantage of 22%–72% of the H coils (#8, 9, 12–14) over the 70-mm Magstim figure-8 coil (#31), at the expense of $S_{1/2}$ increase of 406%–811%. Our results may help interpret studies that claim no significant depth advantage of an H coil (#8) over a 70-mm figure-8 coil (#31).[94–96]

The large $S_{1/2}$ of the H coil electric field compared to conventional figure-8 coils could be contributing to increased risk of seizures, consistent with reports of accidental seizure induction with H coils.[84–86,88] On the other hand, the large $S_{1/2}$ of H coils could also

contribute to therapeutic effectiveness, with reported remission rate in depression[80] nearly twice that reported with the Neuronetics ferromagnetic-core figure-8 coil (#34),[144] though stimulation parameters besides the coils differed in the two studies and a head-to-head comparison of the efficacy of these two coils has not been conducted.

Large diameter circular coils (e.g., #16–19) produce more deeply penetrating electric field than the H coils, at the expense of further reduced focality. Large double-cone type coils (#36 and 39) can provide deeper stimulation than the modeled H coils with comparable focality and may be better suited for spatially confined deep TMS. The half-value depth of large double-cone type coils can be increased by widening the opening angle between the two coil wings. As illustrated in Figure 5, the twin coil $d_{1/2}$ increases for opening angles up to 110°, at which point the reverse trend occurs.

Conclusions

We have presented the most comprehensive comparison of TMS coil electric field penetration and focality to date. We showed that the various TMS coils differ markedly in their electric field characteristics, but they all are subject to a consistent depth–focality tradeoff. Specifically, deeper electric field penetration is achieved at the expense of reduced focality. Consequently, coil designs for deep brain TMS are unfocal and may be associated with increased risk of seizures and other side effects. The ease of seizure induction is an advantage in the context of magnetic seizure therapy, but would be considered a disadvantage for subconvulsive applications of TMS. Figure-8 type coils are fundamentally more focal than circular type coils. None of the simulated coils exhibits depth–focality tradeoff better than that of the figure-8 type coils. MRI gradient coils induce more diffuse electric field compared to TMS coils with comparable depth of field penetration. The addition of a ferromagnetic core can change a coil's depth–focality profile depending on the coil geometry and core placement, but does not overcome the depth–focality tradeoff limit of figure-8 type air-core coils.

Understanding the depth–focality tradeoff can help TMS researchers and clinicians to appropriately select coils and interpret TMS studies. Evaluation of novel coil designs with consistent penetration and focality metrics such as half-value depth $d_{1/2}$ and spread $S_{1/2}$ can provide objective comparison among coil designs. Such comparison, potentially coupled with more detailed simulations in realistic head models, would be a logical precursor to clinical investigations with novel coils. Comparison of the $d_{1/2}$ and $S_{1/2}$ metrics could also be useful in interpreting the differential clinical efficacy and side effects reported with different coils. This study illustrates the utility of computational modeling to inform coil design for various applications of TMS and magnetic seizure therapy.

Supplementary Material

Refer to Web version on PubMed Central for supplementary material.

References

1. Fitzgerald PB, Daskalakis ZJ. The effects of repetitive transcranial magnetic stimulation in the treatment of depression. Expert Rev Med Devices. 2011; 8:85–95. [PubMed: 21158543]
2. Fitzgerald PB, Fountain S, Daskalakis ZJ. A comprehensive review of the effects of rTMS on motor cortical excitability and inhibition. Clin Neurophysiol. 2006; 117:2584–2596. [PubMed: 16890483]
3. Deng, Z-D.; Peterchev, AV.; Lisanby, SH. Coil design considerations for deep-brain transcranial magnetic stimulation (dTMS). Conf Proc IEEE Eng Med Biol Soc; 2008. p. 5675-5679.

4. Krings T, Buchbinder BR, Butler WE, Chiappa KH, Jiang HJ, Rosen BR, et al. Stereotactic transcranial magnetic stimulation: correlation with direct electrical cortical stimulation. Neurosurgery. 1997; 41:1319–1325. [PubMed: 9402583]
5. Tofts PS. The distribution of induced currents in magnetic stimulation of the nervous system. Phys Med Biol. 1990; 35:1119–1128. [PubMed: 2217537]
6. Branston NM, Tofts PS. Analysis of the distribution of currents induced by a changing magnetic field in a volume conductor. Phys Med Biol. 1991; 36:161–168.
7. Esselle KP, Stuchly MA. Neural stimulation with magnetic fields: analysis of induced electric fields. IEEE Trans Biomed Eng. 1992; 39:693–700. [PubMed: 1516936]
8. Jalinous R. Technical and practical aspects of magnetic nerve stimulation. J Clin Neurophysiol. 1991; 8:10–25. [PubMed: 2019644]
9. Ravazzani P, Ruohonen J, Grandori F, Tognola G. Magnetic stimulation of the nervous system: induced electric field in unbounded, semi-infinite, spherical, and cylindrical media. Ann Biomed Eng. 1996; 24:606–616. [PubMed: 8886241]
10. Roth BJ, Cohen LG, Hallett M, Friauf W, Basser PJ. A theoretical calculation of the electric field induced by magnetic stimulation of a peripheral nerve. Muscle Nerve. 1990; 13:734–741. [PubMed: 2385260]
11. Ruohonen, J. PhD dissertation. Espoo, Finland: Department of Engineering Physics and Mathematics, Helsinki University of Technology; 1998. Transcranial magnetic stimulation: modelling and new techniques.
12. Zimmermann KP, Simpson RK. “Slinky” coils for neuromagnetic stimulation. Electroencephalogr Clin Neurophysiol. 1996; 101:145–152. [PubMed: 8647019]
13. Eaton H. Electric field induced in a spherical volume conductor from arbitrary coils: application to magnetic stimulation and MEG. Med Biol Eng Comput. 1992; 30:433–440. [PubMed: 1487945]
14. De Leo R, Cerri G, Balducci D, Moglie F, Scarpino O, Guidi M. Computer modelling of brain cortex excitation by magnetic field pulses. J Med Eng Technol. 1992; 16:149–156. [PubMed: 1433245]
15. Saypol JM, Roth BJ, Cohen LG, Hallett M. A theoretical comparison of electric and magnetic stimulation of the brain. Ann Biomed Eng. 1991; 19:317–328. [PubMed: 1928873]
16. Sekino M, Ueno S. Comparison of current distributions in electroconvulsive therapy and transcranial magnetic stimulation. J Appl Phys. 2002; 91:8730–8732.
17. Sekino M, Ueno S. FEM-based determination of optimum current distribution in transcranial magnetic stimulation as an alternative to electroconvulsive therapy. IEEE Trans Magn. 2004; 40:2167–2169.
18. Kowalski T, Silny J, Buchner H. Current density threshold for the stimulation of neurons in the motor cortex area. Bioelectromagnetics. 2002; 23:421–428. [PubMed: 12210560]
19. Toschi N, Welt T, Guerrisi M, Keck ME. Transcranial magnetic stimulation in heterogeneous brain tissue: clinical impact on focality, reproducibility and true sham stimulation. J Psychiatr Res. 2009; 43:255–264. [PubMed: 18514227]
20. Toschi N, Welt T, Guerrisi M, Keck ME. A reconstruction of the conductive phenomena elicited by transcranial magnetic stimulation in heterogeneous brain tissue. Physica Medica. 2008; 24:80–86. [PubMed: 18296093]
21. Salinas FS, Lancaster JL, Fox PT. Detailed 3D models of the induced electric field of transcranial magnetic stimulation coils. Phys Med Biol. 2007; 52:2879–2892. [PubMed: 17473357]
22. Maccabee PJ, Amassian VE, Eberle LP, Cracco RQ. Magnetic coil stimulation of straight and bent amphibian and mammalian peripheral nerve in vitro: locus of excitation. J Physiol. 1993; 460:201–219. [PubMed: 8487192]
23. Tay G, Chilbert M, Battocletti J, Sances A Jr, Swiontek T, Kurakami C. Measurement of magnetically induced current density in saline in vivo. Conf Proc IEEE Eng Med Biol Soc. 1989; 4:1167–1168.
24. Wagner TA, Gangitano M, Romero R, Theoret H, Kobayashi M, Anschel D, et al. Intracranial measurement of current densities induced by transcranial magnetic stimulation in the human brain. Neurosci Lett. 2004; 354:91–94. [PubMed: 14698446]

25. Tay G, Chilbert MA, Battocletti J, Sances AJ, Swiontek T. Mapping of current densities induced in vivo during magnetic stimulation. Conf Proc IEEE Eng Med Biol Soc. 1991; 13:851–852.
26. Thielscher A, Kammer T. Electric field properties of two commerical figure-8-coils in TMS: calculation of focality and efficiency. Clin Neurophysiol. 2004; 115:1697–1708. [PubMed: 15203072]
27. Lontis ER, Voigt M, Struijk JJ. Focality assessment in transcranial magnetic stimulation with double and cone coils. J Clin Neurophysiol. 2006; 23:463–472.
28. Epstein CM, Davey KR. Iron-core coils for transcranial magnetic stimulation. J Clin Neurophysiol. 2002; 19:376–381. [PubMed: 12436092]
29. Mayberg HS. Targeted electrode-based modulation of neural circuits for depression. J Clin Invest. 2009; 119:717–725. [PubMed: 19339763]
30. Mayberg HS, Lozano AM, Voon V, McNeely HE, Seminowicz D, Hamani C, et al. Deep brain stimulation for treatment-resistant depression. Neuron. 2005; 45:651–660. [PubMed: 15748841]
31. Heller L, van Hulsteyn DB. Brain stimulation using electromagnetic sources: theoretical aspects. Biophys J. 1992; 63:129–138. [PubMed: 1420862]
32. Cohen D, Cuffin BN. Developing a more focal magnetic stimulator. Part I: Some basic principles. J Clin Neurophysiol. 1991; 8:102–111. [PubMed: 2019645]
33. Ruohonen, J.; Ilmoniemi, RJ. Physical principles for transcranial magnetic stimulation. In: Pascual-Leone, A.; Davey, NJ.; Rothwell, J., et al., editors. Handbook of Transcranial Magnetic Stimulation. London: Arnold; 2002. p. 18-30.
34. Grandori F, Ravazzani P. Magnetic stimulation of the motor cortex--theoretical considerations. IEEE Trans Biomed Eng. 1991; 38:180–191. [PubMed: 2066128]
35. Rösler KM, Hess CW, Heckmann R, Ludin HP. Significance of shape and size of the stimulating coil in magnetic stimulation of the human motor cortex. Neurosci Lett. 1989; 100:347–352. [PubMed: 2761784]
36. Rossi S, Hallett M, Rossini PM, Pascual-Leone A. Safety of TMS Consensus Group. Safety, ethical considerations, and application guidelines for the use of transcranial magnetic stimulation in clinical practice and research. Clin Neurophysiol. 2009; 120:2008–2039. [PubMed: 19833552]
37. Barker AT, Jalinous R, Freeston IL. Non-invasive magnetic stimulation of human motor cortex. Lancet. 1985; 1:1106–1107. [PubMed: 2860322]
38. Barker AT. An introduction to the basic principles of magnetic nerve stimulation. J Clin Neurophysiol. 1991; 8:26–37. [PubMed: 2019648]
39. Cadwell J. Optimizing magnetic stimulator design. Electroencephalogr Clin Neurophysiol Suppl. 1991; 43:238–248. [PubMed: 1773761]
40. Hsiao IN, Lin VW. Improved coil design for functional magnetic stimulation of expiratory muscles. IEEE Trans Biomed Eng. 2001; 48:684–694. [PubMed: 11396598]
41. Ruohonen J, Virtanen J, Ilmoniemi R. Coil optimization for magnetic brain stimulation. Ann Biomed Eng. 1997; 25:840–849. [PubMed: 9300108]
42. Di Barba P, Mognaschi ME, Savini A. Synthesizing a field source for magnetic stimulation of peripheral nerves. IEEE Trans Magn. 2007; 43:4023–4029.
43. Cohen LG, Roth BJ, Nilsson J, Dang N, Panizza M, Bandinelli S, et al. Effects of coil design on delivery of focal magnetic stimulation. Technical considerations. Electroencephalogr Clin Neurophysiol. 1990; 75:350–357. [PubMed: 1691084]
44. Ueno S, Tashiro T, Harada K. Localized stimulation of neural tissues in the brain by means of a paired configuration of time-varying magnetic fields. J Appl Phys. 1988; 64:5862–5864.
45. Cuffin BN, Cohen D. Comparison of the magnetoencephalogram and electroencephalogram. Electroencephalogr Clin Neurophysiol. 1979; 47:132–146. [PubMed: 95707]
46. Yunokuchi K, Cohen D. Developing a more focal magnetic stimulator. Part II: Fabricating coils and measuring induced current distributions. J Clin Neurophysiol. 1991; 8:112–120. [PubMed: 2019646]
47. Roth BJ, Turner R, Cohen LG, Hallett M. New coil design for magnetic stimulation with improved focality. Mov Disord. 1990; 5:S32.

48. Ruohonen J, Ravazzani P, Grandori F. Functional magnetic stimulation: theory and coil optimization. Bioelectrochem Bioenerg. 1998; 47:213–219.
49. Roth BJ, Maccabee PJ, Eberle LP, Amassian VE, Hallett M, Cadwell J, et al. In vitro evaluation of a 4-leaf coil design for magnetic stimulation of peripheral nerve. Electroencephalogr Clin Neurophysiol. 1994; 93:68–74. [PubMed: 7511524]
50. Hsu K-H, Nagarajan SS, Durand DM. Analysis of efficiency of magnetic stimulation. IEEE Trans Biomed Eng. 2003; 50:1276–1285. [PubMed: 14619998]
51. Wang X-X, Hu W-P, Yang Y-X, Liang D-D, Zhou J-L, Lu X-C. Computation of depth induced electric field distribution in the magnetic stimulation. Chinese Journal of Medical Physics. 2005; 22:660–662. 634.
52. Ren C, Tarjan PP, Popovic DB. A novel electric design for electromagnetic stimulation-the Slinky coil. IEEE Trans Biomed Eng. 1995; 42:918–925. [PubMed: 7558066]
53. Lin VW, Hsiao IN, Dhaka V. Magnetic coil design considerations for functional magnetic stimulation. IEEE Trans Biomed Eng. 2000; 47:600–610. [PubMed: 10851804]
54. Krasteva VT, Papazov SP, Daskalov IK. Magnetic stimulation for non-homogeneous biological structures. Biomed Eng Online. 2002:1. [PubMed: 12437767]
55. Hu W, Wang X, Yang Y, Liang D, Zhao F. Design of a half solenoid coil for optimization of magnetic focusing in trans-cranial magnetic stimulation. Sheng Wu Yi Xue Gong Cheng Xue Za Zhi. 2007; 24:910–913. [PubMed: 17899772]
56. Knäulein, R.; Weyh, T. Minimization of energy stored in the magnetic field of air coils for medical application. 3rd International Workshop on Electric and Magnetic Fields; 1996. p. 477-482.
57. Liu Z, Yin T, Guan X. A project of magnetic coils newly designed to restrain the negative value of the intensity of magnetic induced electric field. Sheng Wu Yi Xue Gong Cheng Xue Za Zhi. 2003; 20:45–48. 59. [PubMed: 12744160]
58. Ai Q, Li J, Li M, Jiang W, Wang B. A new transcranial magnetic stimulation coil design to improve the focality. BMEI. 2010:1391–1395.
59. Kato, T.; Sekino, M.; Matsuzaki, T.; Nishikawa, A.; Saitoh, Y.; Ohsaki, H. Fabrication of a prototype magnetic stimulator equipped with eccentric spiral coils. Conf Proc IEEE Eng Med Biol Soc; 2011. p. 1985-1988.
60. Hsu KH, Durand DM. A 3-D differential coil design for localized magnetic stimulation. IEEE Trans Biomed Eng. 2001; 48:1162–1168. [PubMed: 11585040]
61. Cret L, Plesa M, Stet D, Ciupa RV. Magnetic coils design for localized stimulation. IFMBE Proceedings. 2007; 16:665–668.
62. Talebinejad, M.; Musallam, S. Effects of TMS coil geometry on stimulation specificity. Conf Proc IEEE Eng Med Biol Soc; 2010. p. 1507-1510.
63. Talebinejad, M.; Musallam, S.; Marble, AE. A transcranial magnetic stimulation coil using rectangular braided litz wire. IEEE International Symposium on Medical Application and Instrumentation; 2011. p. 280-283.
64. Gasca, F.; Richter, L.; Schweikard, A. Simulation of a conductive shield plate for the focalization of transcranial magnetic stimulation in the rat. Conf Proc IEEE Eng Med Biol Soc; 2010. p. 1593-1596.
65. Kim D-H, Georghiou GE, Won C. Improved field localization in transcranial magnetic stimulation of the brain with the utilization of a conductive shield plate in the stimulator. IEEE Trans Biomed Eng. 2006; 53:720–725. [PubMed: 16602579]
66. Kim D-H, Won C, Georghiou GE. Assessment of the sensitivity to field localization of various parameters during transcranial magnetic stimulation. IEEE Trans Magn. 2007; 43:4016–4022.
67. Lu M, Ueno S. Calculating the electric field in real human head by transcranial magnetic stimulation with shield plate. J Appl Phys. 2009; 105:07B322.
68. Davey KR, Riehl ME. Suppressing the surface field during transcranial magnetic stimulation. IEEE Trans Biomed Eng. 2006; 53:190–194. [PubMed: 16485747]
69. Hernandez-Garcia L, Hall T, Gomez L, Michielssen E. A numerically optimized active shield for improved transcranial magnetic stimulation targeting. Brain Stimul. 2010; 3:218–225. [PubMed: 20965451]

70. Kim D-H, Loukaides N, Sykulski JK, Georghious GE. Numerical investigation of the electric field distribution induced in the brain by transcranial magnetic stimulation. IEE Proc Sci Meas Tech. 2004; 151:479–483.
71. Terao Y, Ugawa Y, Sakai K, Uesaka Y, Kohara N, Kanazawa I. Transcranial stimulation of the leg area of the motor cortex in humans. Acta Neurol Scand. 1994; 89:378–383. [PubMed: 8085437]
72. Hayward G, Mehta MA, Harmer C, Spinks TJ, Grasby PM, Goodwin GM. Exploring the physiological effects of double-cone coil TMS over the medial frontal cortex on the anterior cingulate cortex: an H2(15)O PET study. Eur J Neurosci. 2007; 25:2224–2233. [PubMed: 17439499]
73. Lisanby SH, Schlaepfer TE, Fisch HU, Sackeim HA. Magnetic seizure therapy of major depression. Arch Gen Psychiatry. 2001; 58:303–305. [PubMed: 11231838]
74. Roth Y, Zangen A, Mark H. A coil design for transcranial magnetic stimulation of deep brain regions. J Clin Neurophysiol. 2002; 19:361–370. [PubMed: 12436090]
75. Zangen A, Roth Y, Voller B, Hallett M. Transcranial magnetic stimulation of deep brain regions: evidence for efficacy of the H-coil. Clin Neurophysiol. 2005; 116:775–779. [PubMed: 15792886]
76. Roth Y, Amir A, Levkovitz Y, Zangen A. Three-dimensional distribution of the electric field induced in the brain by transcranial magnetic stimulation using figure-8 and deep H-coils. J Clin Neurophysiol. 2007; 24:31–38. [PubMed: 17277575]
77. Roth, Y.; Padberg, F.; Zangen, A. Transcranial magnetic stimulation of deep brain regions: principles and methods. In: Marcolin, MA.; Padberg, F., editors. Transcranial Brain Stimulation for Treatment of Psychiatric Disorders. Vol. 23. Basel: Karger; 2007.
78. Salvador, R.; Miranda, PC.; Roth, Y.; Zangen, A. High-permeability core coils for transcranial magnetic stimulation of deep brain regions. Conf Proc IEEE Eng Med Biol Soc; 2007. p. 6652-6655.
79. Salvador R, Miranda PC, Roth Y, Zangen A. High permeability cores to optimize the stimulation of deeply located brain regions using transcranial magnetic stimulation. Phys Med Biol. 2009; 54:3113–3128. [PubMed: 19420425]
80. Levkovitz Y, Harel EV, Roth Y, Braw Y, Most D, Katz LN, et al. Deep transcranial magnetic stimulation over the prefrontal cortex: evaluation of antidepressant and cognitive effects in depressive patients. Brain Stimul. 2009; 2:188–200. [PubMed: 20633419]
81. Levkovitz Y, Roth Y, Harel EV, Braw Y, Sheer A, Zangen A. A randomized controlled feasibility and safety study of deep transcranial magnetic stimulation. Clin Neurophysiol. 2007; 118:2730–2744. [PubMed: 17977787]
82. Rosenberg O, Shoenfeld N, Zangen A, Kotler M, Dannon PN. Deep TMS in a resistant major depressive disorder: a brief report. Depress Anxiety. 2010; 27:465–469. [PubMed: 20455247]
83. Rosenberg O, Zangen A, Stryjer R, Kotler M, Dannon PN. Response to deep TMS in depressive patients with previous electroconvulsive treatment. Brain Stimul. 2010; 3:211–217. [PubMed: 20965450]
84. Harel EV, Zangen A, Roth Y, Reti I, Braw Y, Levkovitz Y. H-coil repetitive transcranial magnetic stimulation for the treatment of bipolar depression: an add-on, safety and feasibility study. World J Biol Psychiatry. 2011; 12:119–126. [PubMed: 20854181]
85. Rosenberg O, Isserles M, Levkovitz Y, Kotler M, Zangen A, Dannon PN. Effectiveness of a second deep TMS in depression: a brief report. Prog Neuropsychopharmacol Biol Psychiatry. 2011; 35:1041–1044. [PubMed: 21354242]
86. Isserles M, Rosenberg O, Dannon P, Levkovitz Y, Kotler M, Deutsch F, et al. Cognitive-emotional reactivation during deep transcranial magnetic stimulation over the prefrontal cortex of depressive patients affects antidepressant outcome. J Affect Disord. 2011; 128:235–242. [PubMed: 20663568]
87. Levkovitz Y, Sheer A, Harel EV, Katz LN, Most D, Zangen A, et al. Differential effects of deep TMS of the prefrontal cortex on apathy and depression. Brain Stimul. 2011; 4:266–274. [PubMed: 22032742]
88. Levkovitz Y, Rabany L, Harel EV, Zangen A. Deep transcranial magnetic stimulation add-on for treatment of negative symptoms and cognitive deficits of schizophrenia: a feasibility study. Int J Neuropsychopharmacol. 2011; 12:991–996. [PubMed: 21524336]

89. Rosenberg O, Roth Y, Kotler M, Zangen A, Dannon P. Deep transcranial magnetic stimulation for the treatment of auditory hallucinations: a preliminary open-label study. Ann Gen Psychiatry. 2011; 10:3. [PubMed: 21303566]

90. Kranz G, Shamim EA, Lin PT, Kranz GS, Hallett M. Transcranial magnetic brain stimulation modulates blepharospasm: a randomized controlled study. Neurology. 2010; 75:1465–1471. [PubMed: 20956792]

91. Enticott PG, Kennedy HA, Zangen A, Fitzgerald PB. Deep repetitive transcranial magnetic stimlation associated with improved social functioning in a young woman with an autism spectrum disorder. J ECT. 2011; 27:41–43. [PubMed: 20966773]

92. Tartaglia G, Gabriele M, Frasca V, Pichiorri F, Giacomelli E, Cambieri C, et al. Pain relief by deep repetitive transcranial magnetic stimulation applied with the H-coil. Clin Neurophysiol. 2011; 122:S144.

93. Dalla Libera D, Colombo B, Coppi E, Straffi L, Chieffo R, Spagnolo F, et al. Effects of high-frequency repetitive transcranial magnetic stimulation (rTMS) applied with H-coil for chronic migraine prophylaxis. Clin Neurophysiol. 2011; 122:S145–146.

94. Fadini T, Matthäus L, Rothkegel H, Sommer M, Tergau F, Schweikard A, et al. H-coil: induced electric field properties and input/output curves on healthy volunteers, comparison with a standard figure-of-eight coil. Clin Neurophysiol. 2009; 120:1174–1182. [PubMed: 19433366]

95. Roth Y, Pell GS, Zangen A. Motor evoked potential latency, motor threshold and electric field measurements as indices of transcranial magnetic stimulation depth. Clin Neurophysiol. 2010; 121:255–258. [PubMed: 19815456]

96. Fadini T, Matthäus L, Rothkegel H, Sommer M, Tergau F, Schweikard A, et al. Reply to “Motor evoked potential latency, motor threshold and electric field measurements as indices of transcranial magnetic stimulation depth”. Clin Neurophysiol. 2010; 121:258–259.

97. Al-Mutawaly N, de Bruin H, Findlay RD. Magnetic nerve stimulation: field focality and depth of penetration. Conf Proc IEEE Eng Med Biol Soc. 2001; 1:877–880.

98. Crowther LJ, Marketos P, Williams PI, Melikhov Y, Jiles DC, Starzewski JH. Transcranial magnetic stimulation: improved coil design for deep brain investigation. J Appl Phys. 2011; 109:07B314.

99. Ishii K, Matsuzaka Y, Izumi S, Abe T, Nakazato N, Okita T, et al. Evoked motor response following deep transcranial magnetic stimulation in a cynomolgus monkey. Brain Stimul. 2008; 1:300.

100. Volkow ND, Tomasi D, Wang GJ, Fowler JS, Telang F, Wang R, et al. Effects of low-field magnetic stimulation on brain glucose metabolism. NeuroImage. 2010; 51:623–628. [PubMed: 20156571]

101. Carlezon WAJ, Rohan ML, Mague SD, Meloni EG, Parsegian A, Cayetano K, et al. Antidepressant-like effects of cranial stimulation within a low-energy magnetic field in rats. Biol Psychiatry. 2005; 57:571–576. [PubMed: 15780843]

102. Rohan M, Parow A, Stoll AL, Demopulos C, Friedman S, Dager S, et al. Low-field magnetic stimulation in bipolar depression using an MRI-based stimulator. Am J Psychiatry. 2004; 161:93–98. [PubMed: 14702256]

103. Ruohonen J, Ilmoniemi R. Focusing and targeting of magnetic brain stimulation using multiple coils. Med Biol Eng Comput. 1998; 36:297–301. [PubMed: 9747568]

104. Ruohonen J, Ravazzani P, Grandori F, Ilmoniemi RJ. Theory of multichannel magnetic stimulation: toward functional neuromuscular rehabilitation. IEEE Trans Biomed Eng. 1999; 46:646–651. [PubMed: 10356871]

105. Ho SL, Xu GZ, Fu WN, Yang QX, Hou HJ, Yan WL. Optimization of array magnetic coil design for functional magnetic stimulation based on improved genetic algorithm. IEEE Trans Magn. 2009; 45:4849–4852.

106. Lu M, Ueno S, Thorlin T, Persson M. Calculating the current density and electric field in human head by multichannel transcranial magnetic stimulation. IEEE Trans Magn. 2009; 45:1662–1665.

107. Han BH, Chun IK, Lee SC, Lee SY. Multichannel magnetic stimulation system design considering mutual couplings among the stimulation coils. IEEE Trans Biomed Eng. 2004; 51:812–817. [PubMed: 15132507]

108. Wang XM, Chen Y, Guo MX, Wang MS. Finite-element simulation for magnetic fields created by multi-channel brain magnetic stimulator. Acta Biophysica Sinica. 2005; 21:377–384.
109. Wang X, Chen Y, Guo M, Wang M. Design of multi-channel brain magnetic stimulator and ANSYS simulation. IJBEM. 2005; 7:259–262.
110. Yang S, Xu G, Wang L, Geng Y, Yu H, Yang Q. Circular coil array model for transcranial magnetic stimulation. IEEE Trans Appl Supercond. 2010; 20:829–833.
111. Cao X, Cai D, Zhang X, Liu R, Tang J. Optimization of electric field distribution of multichannel transcranial magnetic stimulation based on genetic algorithm. BMEI. 2010:1544–1547.
112. Guo M-X, Wang X-M, Wang M-S. Design of the coil array and calculation of the field distribution of transcranial brain multichannel magnetic stimulation. Journal of Tianjin Medical University. 2001; 7:38–40.
113. Im CH, Lee C. Computer-aided performance evaluation of a multichannel transcranial magnetic stimulation system. IEEE Trans Magn. 2006; 42:3803–3808.
114. Xu G, Chen Y, Yang S, Wang M, Yan W. The optimal design of magnetic coil in transcranial magnetic stimulation. Conf Proc IEEE Eng Med Biol Soc. 2006; 6:6221–6224. [PubMed: 17281687]
115. Lee C, Im C-H, Jung H-K. Analysis and design of whole-head magnetic brain stimulators: a simulation study. International Journal of Control, Automation, and Systems. 2007; 5:337–342.
116. Huang YZ, Sommer M, Thickbroom G, Hamada M, Pascual-Leonne A, Paulus W, et al. Consensus: new methodologies for brain stimulation. Brain Stimul. 2009; 2:2–13. [PubMed: 20633398]
117. Nadeem M, Thorlin T, Gandhi OP, Persson MA. Computation of electric and magnetic stimulation in human head using the 3-D impedance method. IEEE Trans Biomed Eng. 2003; 50:900–907. [PubMed: 12848358]
118. Wagner TA, Zahn M, Grodzinsky AJ, Pascual-Leone A. Three-dimensional head model simulation of transcranial magnetic stimulation. IEEE Trans Biomed Eng. 2004; 51:1586–1598. [PubMed: 15376507]
119. Chen M, Mogul DJ. A structurally detailed finite element human head model for simulation of transcranial magnetic stimulation. J Neurosci Methods. 2009; 179:111–120. [PubMed: 19428517]
120. Opitz A, Windhoff M, Heidemann RM, Turner R, Thielscher A. How the brain tissue shapes the electric field induced by transcranial magnetic stimulation. NeuroImage. 2011; 58:849–859. [PubMed: 21749927]
121. Thielscher A, Opitz A, Windhoff M. Impact of the gyral geometry on the electric field induced by transcranial magnetic stimulation. NeuroImage. 2011; 54:234–243. [PubMed: 20682353]
122. Roth BJ, Saypol JM, Hallett M, Cohen LG. A theoretical calculation of the electric field induced in the cortex during magnetic stimulation. Electroencephalogr Clin Neurophysiol. 1991; 81:47–56. [PubMed: 1705219]
123. Deng Z-D, Lisanby SH, Peterchev AV. Electric field strength and focality in electroconvulsive therapy and magnetic seizure therapy: a finite element simulation study. J Neural Eng. 2011; 8:016007. [PubMed: 21248385]
124. Davey KR, Epstein CM, George MS, Bohning DE. Modeling the effects of electrical conductivity of the head on the induced electric field in the brain during magnetic stimulation. Clin Neurophysiol. 2003; 114:2204–2209. [PubMed: 14580620]
125. Thielscher A, Kammer T. Linking physics and physiology in TMS: a sphere field model to determine the cortical stimulation site in TMS. NeuroImage. 2002; 17:1117–1130. [PubMed: 12414254]
126. Thielscher A, Wichmann FA. Determining the cortical target of transcranial magnetic stimulation. NeuroImage. 2009; 47:1319–1330. [PubMed: 19371785]
127. Deng Z-D, Lisanby SH, Peterchev AV. Comparative electric field characteristics of deep transcranial magnetic stimulation coils. Clin Neurophysiol. 2011; 122:S189.
128. Epstein CM, Schwartzberg DG, Davey KR, Sudderth DB. Localizing the site of magnetic brain stimulation in humans. Neurology. 1990; 40:666–670. [PubMed: 2320243]
129. Haus, HA.; Melcher, JR. Electromagnetic Fields and Energy. New Jersey: Printice-Hall; 1989.

130. Krause L, Enticott PG, Zangen A, Fitzgerald PB. The role of medial prefrontal cortex in theory of mind: a deep rTMS study. Behav Brain Res. 2012; 228:87–90. [PubMed: 22155478]
131. Webb JP, Forghani B. T-Ω method using hierarchal edge elements. IEE Proceedings: Science, Measurement and Technology. 1995; 142:133–141.
132. ElecNet/MagNet. 2D/3D electromagnetic field simulation software documentation computer program. Version 7. Montréal, Québec; Canada: 2009.
133. Deng, Z-D.; Lisanby, SH.; Peterchev, AV. Improving the focality of electroconvulsive therapy: the roles of current amplitude, and electrode size and spacing. 20th Annual Meeting of the International Society for Neurostimulation; New Orleans, LO: J ECT; 2010. p. 151
134. Carbunaru R, Durand DM. Toroidal coil models for transcutaneous magnetic simulation of nerves. IEEE Trans Biomed Eng. 2001; 48:434–441. [PubMed: 11322531]
135. Datta A, Elwassif M, Battaglia F, Bikson M. Transcranial current stimulation focality using disc and ring electrode configurations: FEM analysis. J Neural Eng. 2008; 5:163–174. [PubMed: 18441418]
136. Peterchev AV, Wagner TA, Miranda PC, Nitsche MA, Paulus W, Lisanby SH, et al. Fundamentals of transcranial electric and magnetic stimulation dose: definition, selection, and reporting practices. Brain Stimul. 2012 AIP.
137. Balslev D, Braet W, McAllister C, Miall RC. Inter-individual variability in optimal current direction for transcranial magnetic stimulation of the motor cortex. J Neurosci Methods. 2007; 162:309–313. [PubMed: 17353054]
138. Di Lazzaro V, Oliviero A, Mazzone P, Insola A, Pilato F, Saturno E, et al. Comparison of descending volleys evoked by monophasic and biphasic magnetic stimulation of the motor cortex in conscious humans. Exp Brain Res. 2001; 141:121–127. [PubMed: 11685416]
139. Kammer T, Beck S, Thielscher A, Laubis-Herrmann U, Topka H. Motor thresholds in humans: a transcranial magnetic stimulation study comparing different pulse waveforms, current directions and stimulator types. Clin Neurophysiol. 2001; 112:250–258. [PubMed: 11165526]
140. Deng, Z-D.; Lisanby, SH.; Peterchev, AV. Effect of anatomical variability on neural stimulation strength and focality in electroconvulsive therapy (ECT) and magnetic seizure therapy (MST). Conf Proc IEEE Eng Med Biol Soc; 2009. p. 682-688.
141. Weissman JD, Epstein CM, Davey KR. Magnetic brain stimulation and brain size: relevance to animal studies. Electroencephalogr Clin Neurophysiol. 1992; 85:215–219. [PubMed: 1376680]
142. Turner R. Gradient coil design: a review of methods. Magn Reson Imaging. 1993; 11:903–920. [PubMed: 8231676]
143. Deng, Z-D.; Peterchev, AV. Transcranial magnetic stimulation coil with electronically switchable active and sham modes. Conf Proc IEEE Eng Med Biol Soc; 2011. p. 1993-1996.
144. O'Reardon JP, Solvason HB, Janicak PG, Sampson S, Isenberg KE, Nahas Z, et al. Efficacy and safety of transcranial magnetic stimulation in the acute treatment of major depression: a multisite randomized controlled trial. Biol Psychiatry. 2007; 62:1208–1216. [PubMed: 17573044]
145. Tischler H, Wolfus S, Friedman A, Perel E, Pashut T, Lavidor M, et al. Mini-coil for magnetic stimulation in the behaving primate. J Neurosci Methods. 2011; 194:242–251. [PubMed: 20974177]
146. Hovey, C.; Jalinous, R. [Last accessed Nov. 17, 2011.] The Guide to Magnetic Stimulation. 2006. http://www.icts.uci.edu/neuroimaging/GuidetoMagneticStimulation2008.pdf
147. Zangen, A.; Roth, Y.; Miranda, PC.; Hazani, D.; Hallett, M., inventors. Transcranial magnetic stimulation system and methods. World Intellectual Property Organization, WO 2006/134598. Dec 21. 2006 p. A2
148. Rafiroiu D, Vlad S, Cret L, Ciupa RV. 3D modeling of the induced electric field of transcranial magnetic stimulation. IFMBE Proceedings. 2009; 26:333–338.
149. MagVenture A/S. Magnetic Stimulation Accessories Catalogue; Denmark: 2010.
150. Yang S, Xu G, Wang L, Geng D, Yang Q. Electromagnetic field simulation of 3D realistic head model during transcranial magnetic stimulation. ICBBE. 2007:656–659.
151. Ruohonen J, Ollikainen M, Nikouline V, Virtanen J, Ilmoniemi RJ. Coil design for real and sham transcranial magnetic stimulation. IEEE Trans Biomed Eng. 2000; 47:145–148. [PubMed: 10721620]

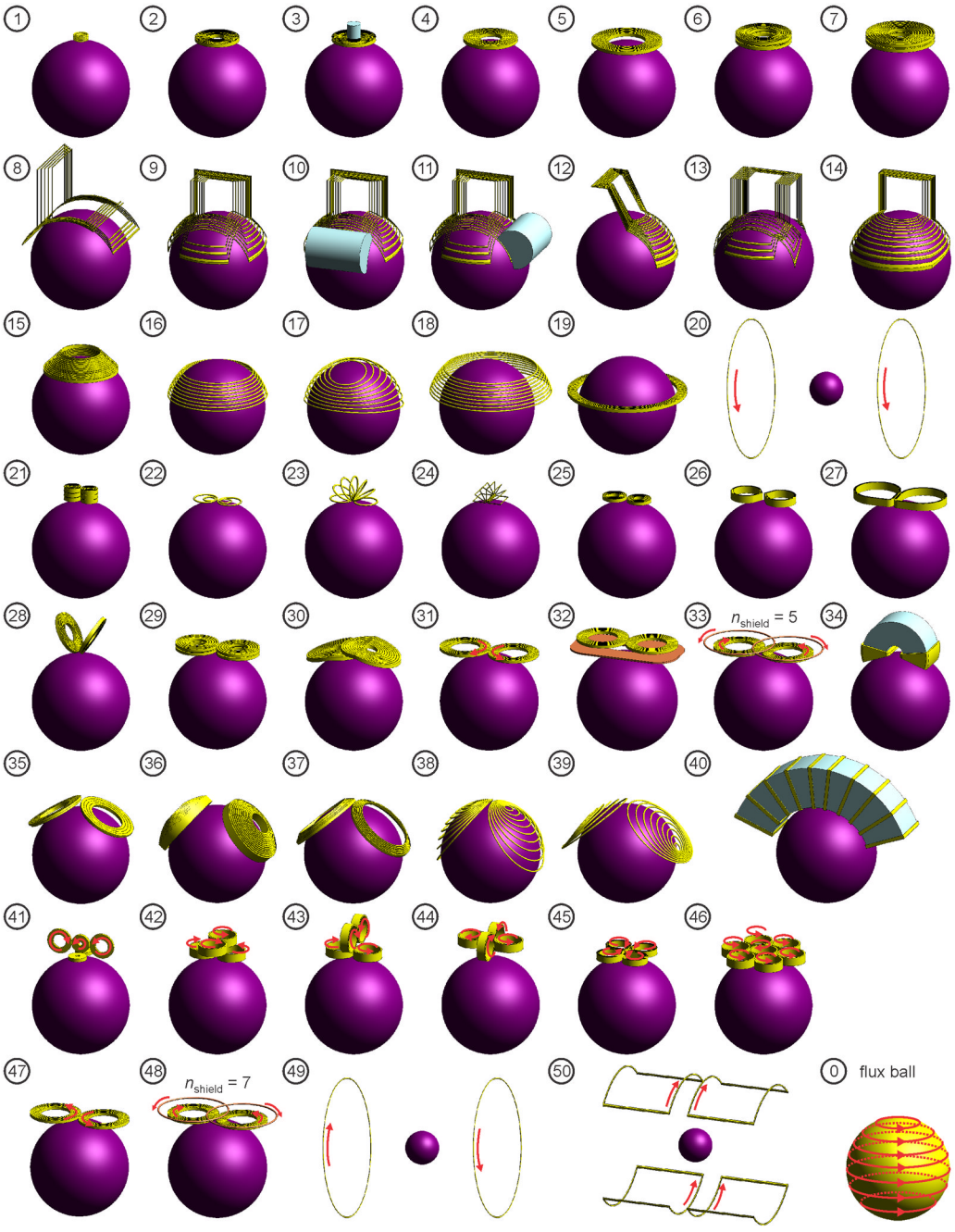

Figure 1.

Simulation models of 50 TMS coil configurations: (1) Animal mini-coil,[145] (2) Magstim 50 mm circular coil (P/N 9999),[146] (3) 50 mm circular coil with iron core,[70] (4) Magstim 70 mm circular coil (P/N 3192),[146] (5) Magstim 90 mm circular coil (P/N 3192),[146] (6) Magstim animal MST coil, (7) Magstim human MST coil (S/N MP39), (8) Brainsway H coil,[147] (9) Brainsway H1 coil,[76,80–83,147] (10) H1 coil with frontal iron core,[79] (11) H1 coil with lateral iron core,[79] (12) Brainsway H1L coil,[80] (13) Brainsway H2 coil,[76,80,81,147] (14) Brainsway HADD coil,[116] (15) Magstim cap coil, (16) crown coil,[3] (17) crown coil with back-splayed winding, (18) crown coil with back-spaced winding, (19) supraorbital halo coil,[98,99] (20) MRI z-gradient coil in parallel-current (Helmholz) mode,[100] (21) 3-layer

double coil,[62] (22) double butterfly,[56,58,59] (23) circular slinky-7 coil,[52,53] (24) rectangular slinky-7 coil,[12,53,54] (25) Magstim 25 mm figure-8 (P/N 1165),[21,146] (26) Cadwell Corticoil,[148] (27) Cadwell B-shaped coil,[21] (28) 50 mm V-coil,[13] (29) MagVenture C-B65 butterfly coil,[149] (30) MagVenture MC-B70 butterfly coil,[26,27,149] (31) Magstim 70 mm figure-8 coil (P/N 9925, 3190),[146] (32) 70 mm figure-8 with shielding plate,[65] (33) 70 mm figure-8 with active shield (5 turns),[69] (34) Neuronetics iron-core figure-8 coil (CRS 2100),[28,68] (35) MagVenture D-B80 butterfly coil,[27,149] (36) MagVenture MST twin coil, (37) Magstim double cone coil (P/N 9902),[146] (38) eccentric double cone coil with center-dense windings, (39) eccentric double cone coil with center-sparse windings, (40) stretched C-core coil,[3,68] (41) 3-D differential coil,[60] (42) 3-D coil array #1,[114] (43) 3-D coil array #2,[114] (44) 3-D coil array #3,[114] (45) Cadwell cloverleaf coil,[48,49] (46) circular coil array,[110,150] (47) Magstim 70 mm figure-8 coil in reversed-current mode,[151] (48) 70 mm figure-8 with active shield (7 turns),[69] (49) MRI z-gradient coil opposing-current (Maxwell) mode,[100] and (50) MRI x- (or y-) gradient (Golay) coil.[102] The last configuration, labeled “0”, is the ideal “flux ball” coil whose windings are parallel to the circles of latitude of the spherical model and cover the whole head.[129]

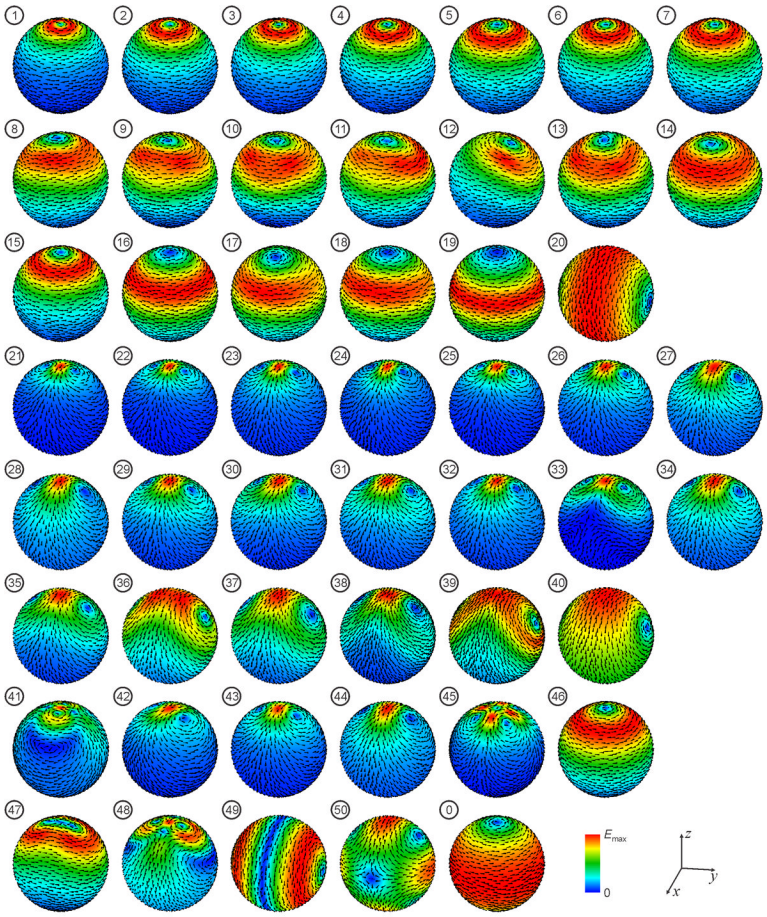

Figure 2.

Induced electric field distribution on the brain surface by the 50 TMS coils from Figure 1. The electric field magnitude is plotted with a color map normalized to the field maximum in the brain, E_{max}, for each coil. The arrows indicate the electric field direction.

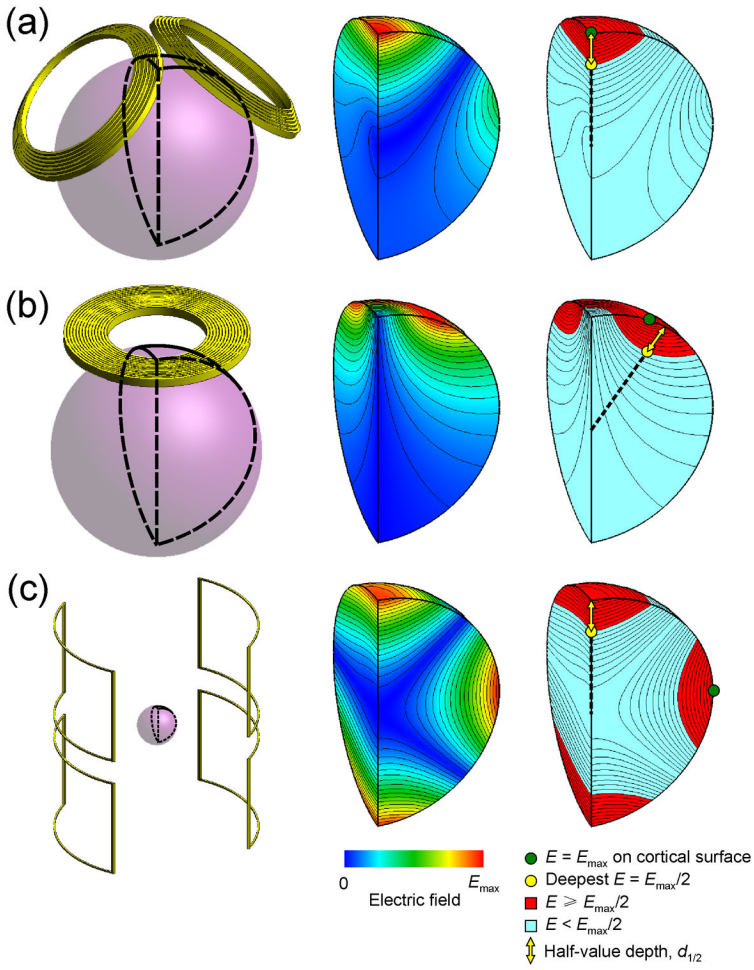

Figure 3.

Examples of electric field characterization for (a) double-cone (#37), (b) 90-mm circular (#5), and (c) MRI x- (or y-) gradient (#50) coils. The left column shows the respective coil and the spherical model representation of the brain. The middle column shows the electric field strength contour and color maps on the quarter-sphere segment of the brain outlined in black on the left. The right column shows the location of the maximum induced electric field on the brain surface, E_{max} (green circle), and the location of the deepest point where the electric field strength is $E_{max}/2$ (yellow circle). Note that the deepest point where $E = E_{max}/2$ does not necessarily fall on the same radial line as E_{max}. The yellow arrow represents the half-value depth, $d_{1/2}$, which is the radial distance from the cortical surface to the deepest point where the electric field strength is half of its maximum value on the cortical surface. The red portions of the quarter-sphere indicate the regions of the brain exposed to electric field as strong as or stronger than $E_{max}/2$; the total volume of these regions is $V_{1/2}$. The half-value spread, $S_{1/2}$, is defined as $S_{1/2} = V_{1/2}/d_{1/2}$.

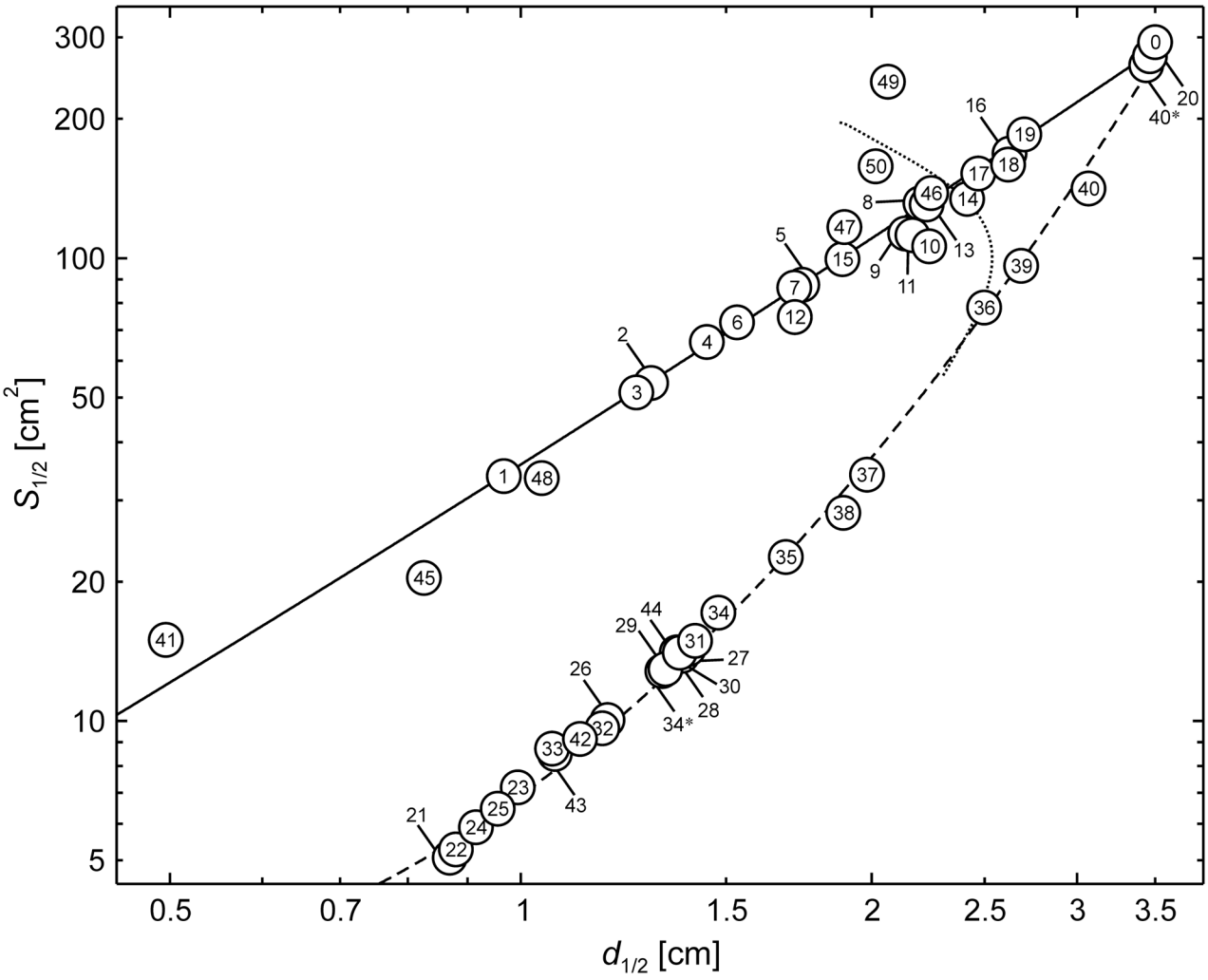

Figure 4.

Electric field focality quantified by the half-value spread, $S_{1/2}$, as a function of the half-value depth, $d_{1/2}$, for the TMS coils in Figure 1. The definitions of metrics $d_{1/2}$ and $S_{1/2}$ are illustrated in Figure 2. The solid and dashed lines are curves of best fit of the points corresponding to symmetric circular (#1–7, 15, 16, 19, and 20) and figure-8 (#21–26, 28, 29, 31, 32, 34–40) type coils, respectively. Coils #34* and #40* are the air-core counterparts to ferromagnetic-core coils #34 and 40, respectively. For large coil sizes the depth–focality tradeoff trends for both circular and figure-8 type coils converge to the flux ball (coil #0) which corresponds to uniform magnetic field in the head and has $S_{1/2}$ = 308 cm^2 and $d_{1/2}$ = 3.5 cm. The dotted line is the $S_{1/2}$ –$d_{1/2}$ locus for the MagVenture MST twin coil (#36) for a range of inter-loop opening angles, replicated from Figure 4.

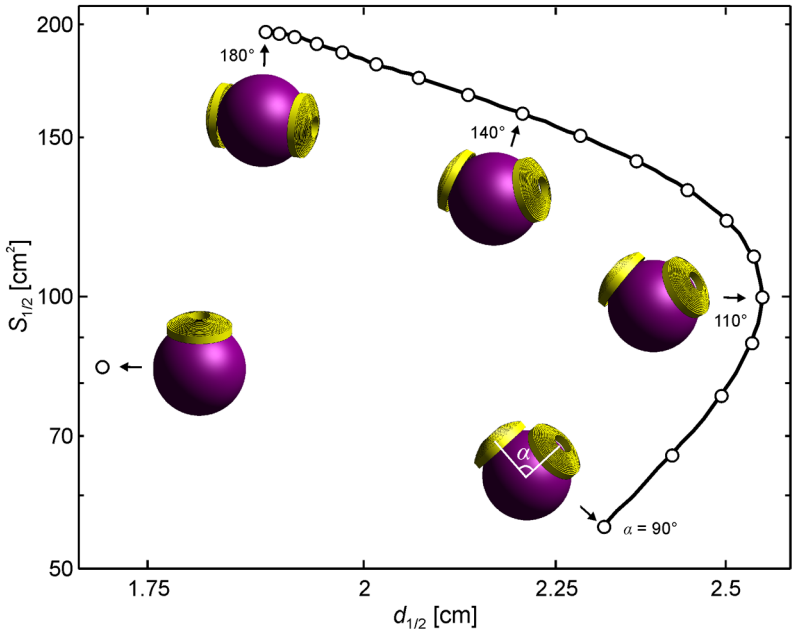

Figure 5.
Electric field $S_{1/2}$ –$d_{1/2}$ locus for the MagVenture MST twin coil (#36) for inter-loop opening angles ranging from 90° to 180°. The field characteristics of one of the twin coil windings is also plotted for comparison.